Pergamon

Tetrahedron, Vol. 53, No. 12, pp. 4317-4330, 1997

0040-4020/97 $17.00 + 0.00

PII: S0040-4020(97)00158-0

Ab Initio Molecular Orbital Study on the Mechanism of Amide Hydrolysis Dependent on Leaving Groups.

Kenzi Hori,*[a] Akio Kamimura,[b] Kaori Ando, Miyuki Mizumura, and Yasuji Ihara[c]

[a]Institute for Fundamental Research of Organic Chemistry,

Kyushu University, Fukuoka 812-81, Japan

[b] Department of Applied Chemistry and Chemical Engineering, Faculty of Engineering, Yamaguchi University, Ube 755, Japan

[c] Yamaguchi Prefectural University, Sakurabatake, Yamaguchi 753, Japan

Abstract: The alkaline hydrolysis of amides, N-methyl acetamide **1**, acetanilide **2**, and N-acetyl imidazole **3**, was investigated by use of *ab initio* molecular orbital calculations. A detailed analysis was performed for two possible mechanisms, Path 1 and 2. Path 1, similar to ester hydrolysis, releases CH_3COOH and RNH^- whereas Path 2 contains the RNH group that extracts the H atom from the OH fragment in the tetrahedral intermediate. In this mechanism, carboxylate ion and an amine directly form. It was ascertained that Path 2 is a better route to decompose the TD intermediate than Path 1 for **1** and **2** in the gas phase. The stability of the leaving group RNH^- determines which route, Path 1 or 2, is preferred in the gas phase. The solvent effect was estimated for the two mechanisms by using the SCRF calculations of the IPCM model. © 1997 Elsevier Science Ltd.

Introduction

The alkaline hydrolysis of esters RC(=O)OR' (Y=OR in Eq. 1) involves the formation of the tetrahedral intermediate (TD) by the reaction of ester and OH^- as shown in Scheme 1. This intermediate easily decomposes into a carboxylic acid and an alkoxide ion (Path 1). The former reaction determines the rate of ester hydrolysis in solution since the OH^- requires large desolvation energy in forming the TD intermediate.[1] On the other hand, in the gas phase, theoretical calculations showed that the latter process, decomposition of the intermediate, needs large activation energy; in fact, it needs more than 20 kcal mol^{-1} in that alkoxide ions are not stable in such a phase.[1,2,3] There is an alternative mechanism (Path 2) that the alkoxide group extracts the H atom from

Scheme I

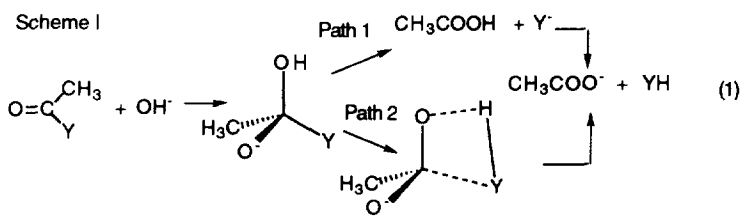

the OH fragment and a carboxylate ion and an alcohol directly form. This was proposed by Takashima et al.[4] based on a finding from their experiments in the gas phase. We calculated the possibility of this mechanism by using *ab initio* molecular orbital (MO) calculations.[2]

A similar mechanism (Path 1) is applicable to the alkaline hydrolysis of amides RC(=O)NHR' (Y=NHR' in Eq. 1).[5] The measurement of the rate constants in *p*-substituted N-methyl acetanilide,[6] trifluoroacetanilide and its derivatives[7] made it possible to discuss the mechanism of their alkaline hydrolysis. The studies, which were done in solution, observed two paths, i.e., with respect to OH^-, one is the second order reaction and the other the first order. Only the first order behavior of OH^- was observed in simple amides such as benzamide[8], toluamides[9] and simple aliphatic amides[10] in solution. Therefore, the stability of RNH^- as a leaving group largely relates to which route is preferred. Paths 1 and 2 are first-order mechanisms with respect to the OH^- concentration although the latter does not form the $R'NH^-$ intermediate. Therefore, they are one of the candidates for the mechanism that has the first order dependence on the OH^- ion. Brown et al. performed detailed mechanistic studies on amide hydrolysis, in which they assert that water is involved in the decomposition of the TD intermediates.[11] They proposed that in their mechanism similar to Path 1 RNH^- extracts a proton of a water as a reactant and surrounding waters act as only a dielectric field.

In the gas phase, the rate determining step is not the TD intermediate formation but its breakdown. Path 1 with an alkyl group as R' is not a good candidate of the TD intermediate decomposition because $R'NH^-$ ion is very unstable and Path 2 may be the better route. On the other hand, if the resonance effect in R' can stabilize the leaving group $R'NH^-$ such as *p*-NO_2-$C_6H_5NH^-$, the anion may be a product. In fact, the leaving group dependence were observed in many experiments in solution. *Ab initio* MO calculations can serve to investigate these mechanisms in the gas phase. There have been a number of theoretical studies dealing with the hydrolysis mechanism of amides and esters.[1,2,3,5,12] In the present study, *ab initio* MO calculations were used to conduct theoretical examination of both Path 1 and Path 2 as plausible mechanisms at work for the breakdown of the TD intermediate in the gas phase. Although limited, it is possible to calculate energies including solvent effect with the SCRF calculations of the isodensity polarized continuum model (IPCM).[13] Therefore, the gas phase mechanisms together with the SCRF calculations will give insight into the hydrolysis mechanism in solution.

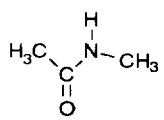

1

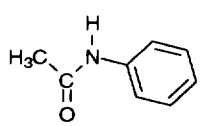

2

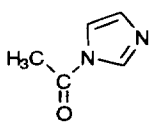

3

In a previous paper using the results of the RHF/6-31G calculations,[14] we discussed the alkaline hydrolysis of N-acetyl imidazole **3**. This molecule is a kind of amide which can release imidazolyl anion, the product of Path 1, and we totally recalculated the energy profiles of this amide using higher basis sets. The reaction mechanisms for **1** and **2** are compared with that for **3** in order to investigate how the leaving group relates to the reaction mechanism of decomposing the TD intermediates in the gas phase and in aqueous solution.

Method of Calculations

MOPAC Ver. 6[15] was used for the preliminary search of potential profiles of the reaction mechanisms

considered here. The *ab initio* MO calculations were done on the GAUSSIAN94 program[16] at the Institute for Molecular Science and workstations in our institute. It is necessary to include diffuse basis functions for geometry optimizations because the molecules calculated here have anion fragments. Therefore, molecular geometries including transition states (TS) were optimized at the RHF/6-31+G level for **1**, **2** and **3**. All the geometries obtained were checked with vibration frequency calculations. The 6-31G basis sets[17] served to optimize the geometry and to calculate the geometry transformation along the intrinsic reaction coordinate (IRC) because the incapability of the larger basis set in our system, especially for **2**.

In order to obtain the energy relations between reactants, intermediates, TS's and products, we defined the difference in the energy of the TD intermediates shown in Figure 1: ΔE_1 is the stabilization energy released by the TD intermediate formation; ΔE_3(TS) the activation energy for Path 1 or 2; ΔE_2 and ΔE_4 energy differences between the TD intermediate and, on one hand, $CH_3COOH + Y^-$, and, the other hand, $CH_3COO^- + YH$, respectively; and lastly, ΔE_5 is defined as the energy difference between amine HY and its anion Y^-,

$$\Delta E_5 = E_{Y^-} - E_{HY} \qquad (2).$$

Both MP2/6-31+G//RHF/6-31G and MP2/6-31+G*//RHF/6-31+G energies were calculated to have better energy description concerning the molecules under consideration. In fact, the calculations by the MP2/6-31+G//RHF/6-31G level underestimated ΔE_1's by ca. 10 kcal mol^{-1} in comparison with those of MP2/6-31+G*//RHF/6-31+G level as seen in Table 2. However, the other energies differed by no more than 4 kcal mol^{-1} between the energies using the 6-31G and the 6-31+G optimized geometries.

The intrinsic reaction coordinates[18] (IRC) were calculated in order to check and obtain energetic and geometric profiles of the proposed reaction mechanism. We adopted 0.02 $amu^{1/2}$ Bohr as the step size for the IRC calculations for **1**, **2**, and **3**. The IRCs for **1** and **3** were also calculated with the 6-31+G basis sets and the 0.01 step size to check the reliability of the RHF/6-31G level of theory. As will be discussed below, the 6-31G calculations for **1** and **3** gave the IRC profiles qualitatively similar to those at the 6-31+G level of theory.

In order to estimate solvent effect for the energy relation, we performed the SCRF calculations of the IPCM model.[13] The geometries optimized in the gas phase were used for the energy estimation. In order to simulate mechanisms in aqueous solution the dielectric constant ε=78.3 was used for the IPCM calculations.

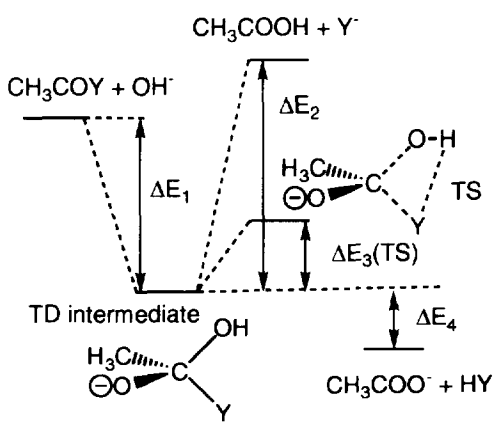

Figure 1 Energy relation diagram for alkaline hydrolysis of amides CH_3COY (Y = $C_3H_3N_2$, C_6H_5NH or CH_3NH)

Table 1 Optimized parameters (in Å and degree units for lengths and angles, respecively) and the total energies (in Hartree Unit) for the TD intermediate and the TS of the three amides.

	1		2		3	
	TD	TS	TD	TS	TD	TS
RHF/6-31G[a]	-322.25942	-322.21853	-512.73230	-512.70771	-451.83119	-451.81915
MP2/6-31+G[a]	-322.94986	-322.91425	-513.85044	-513.83004	-452.80325	-452.79438
RHF/6-31+G[a]	-322.28740	-322.24257	-512.76237	-512.73557	-451.86010	-451.84488
MP2/6-31+G*[a]	-323.36870	-323.33462	-514.53532	-514.52129	-453.42225	-453.41772
MP2/6-31+G*(SCRF)[c]	-323.47073	-323.42909	-514.63247	-514.61147	-453.51578	-453.50905
O(1)-C(2)	1.345(1.329)	1.235(1.234)	1.333(1.322)	1.240(1.236)	1.326(1.313)	1.248(1.246)
C(2)-N(6)	1.455(1.496)	2.194(2.175)	1.491(1.500)	2.118(2.131)	1.515(1.527)	2.013(2.000)
O(4)-H(5)	0.953(0.953)	0.971(1.100)	0.953(0.953)	0.952(0.952)	0.953(0.953)	0.952(0.952)
H(5)-N(6)	2.946(2.935)	1.886(1.814)	2.839(2.815)	2.711(2.702)	2.826(2.803)	2.818(2.800)
∠O(1)-C(2)-O(4)	109.6(110.1)	120.1(120.8)	111.2(111.7)	119.4(119.5)	112.5(115.8)	118.9(122.3)
τ[O(1)-C(2)-C(3)-O(4)]	118.7(121.1)	154.1(154.7)	122.1(122.6)	150.4(151.0)	124.7(125.6)	147.3(146.7)

[a] The lines for RHF/6-31G and RHF/6-31+G lists the total energies estimated from RHF/6-31G and RHF/6-31+G basis set calculations. MP2/6-31+G and MP2/6-31+G* show the total energies of MP2/6-31+G//RHF/6-31G and MP2/6-31+G*//RHF/6-31+G calculations, respectively.

[b] Values in the table are the optimized parameters from the RHF/6-31G (RHF/6-31+G) optimizations.

[b] The SCRF energies at the MP2/6-31+G*//RHF/6-31+G level of theory.

Results and Discussions

Geometries and Energy Relations among Reactants, TSs and Products.

First of all, the TD intermediates for **1**, **2** and **3** were optimized , and then, the their TS geometries were also searched by referring that obtained for methyl acetate.[2] As will be discussed later, the TS geometries obtained for **1** and **2** correspond to those for Path 2 and that for **3** to Path 1. Table 1 summarizes the total energies and the optimized parameters of the TD and TS geometries which are displayed in Figure 2 together with C(2)-N(6) and H(5)-N(6) distances. The calculations of the H(5)-N(6) lengths at the TS for **1**, **2** and **3** turned out to be 1.886 (1.814)[19], 2.711 (2.702) and 2.818 (2.800) Å, respectively: with **1** the N-H distance is much shorter than those with the others. The C(2)-N(6) distances have a trend opposite to the H(5)-N(6) length, i.e., they are 2.194 (2.175), 2.118 (2.131) and 2.013 (2.000) Å, respectively.

The dihedral angle τ[O(1)-C(2)-C(3)-O(4)] indexes the hybridization of the C(2) atom in the CH_3COO fragment; this angle should be around 120° in the TD intermediate and 180° in acetate anion or acetic acid as the product because the C(2) has the sp^3 and sp^2 hybridization, respectively. In the TD intermediate, the angles are 118.7° (121.1°), 122.1° (122.6°), and 124.7° (125.6°) by estimation for **1**, **2** and **3**, respectively. The differences of the angle between TS and TD were calculated to be by 35.4° (33.6°), 28.3° (28.4°), and 22.6° (21.0°), respectively. It follows that the C(2) in the CH_3COO fragment loses the sp^3 nature at the TS in the order of **1>2>3**. These geometrical features such as the H(5)-N(6) and C(2)-N(6) lengths, the hybridization in the C(2) carbon relates to the potential energy profile to a great extent as we will be discussed below.

The energy relations among the structures on the IRC largely associate to the question of which is the preferable mechanism for the decomposition of the TD intermediates, Path 1 or Path 2. The energy relations between **1**, **2** and **3** are summarized in Table 2. The ΔE_1, the stabilization energy due to the TD intermediate formation, was estimated to be 12.1 kcal mol^{-1} for **1** in the MP2/6-31+G//RHF/6-31G level. This value is

Table 2 The energy relation in kcal mol^{-1} unit among the reactants, the TS and the Products along the IRC. The definition of the energies in the table is shown in Figure 1 and in Eq. 2.

	1	**2**	**3**
ΔE_1	21.4 (12.1)	33.5 (24.7)	54.5 (45.5)
ΔE_2	47.2 (50.1)	–[b] (22.3)	7.5 (13.1)
ΔE_3(TS)	21.4 (22.3)	8.8 (12.8)	2.8 (5.6)
ΔE_4	-16.1 (-18.0)	-7.9 (-10.2)	4.1 (3.0)
ΔE_5	409.0 (411.8)	–[b] (376.2)	349.0 (353.8)
ΔE_1(SCRF)	-3.7	5.9	24.2
ΔE_2(SCRF)[c]	33.4	–[b]	-2.4
ΔE_3(TS,SCRF)[c]	26.1	13.2	4.2
ΔE_4(SCRF)[c]	-23.9	-21.3	-13.6

[a] The values in the table were calculated at the MP2/6-31+G*//RHF/6-31+G (MP2/6-31+G//RHF/6-31G) level of theory.

[b] ΔE_2, ΔE_5 and ΔE_2(SCRF) could not obtained in the MP2/6-31+G*//RHF/6-31+G level because of the convergence failure of the anion $C_6H_5NH^-$.

[c] ΔE_2(SCRF) and ΔE_3(TS,SCRF) at the MP2/6-31+G*//RHF/6-31+G level theory.

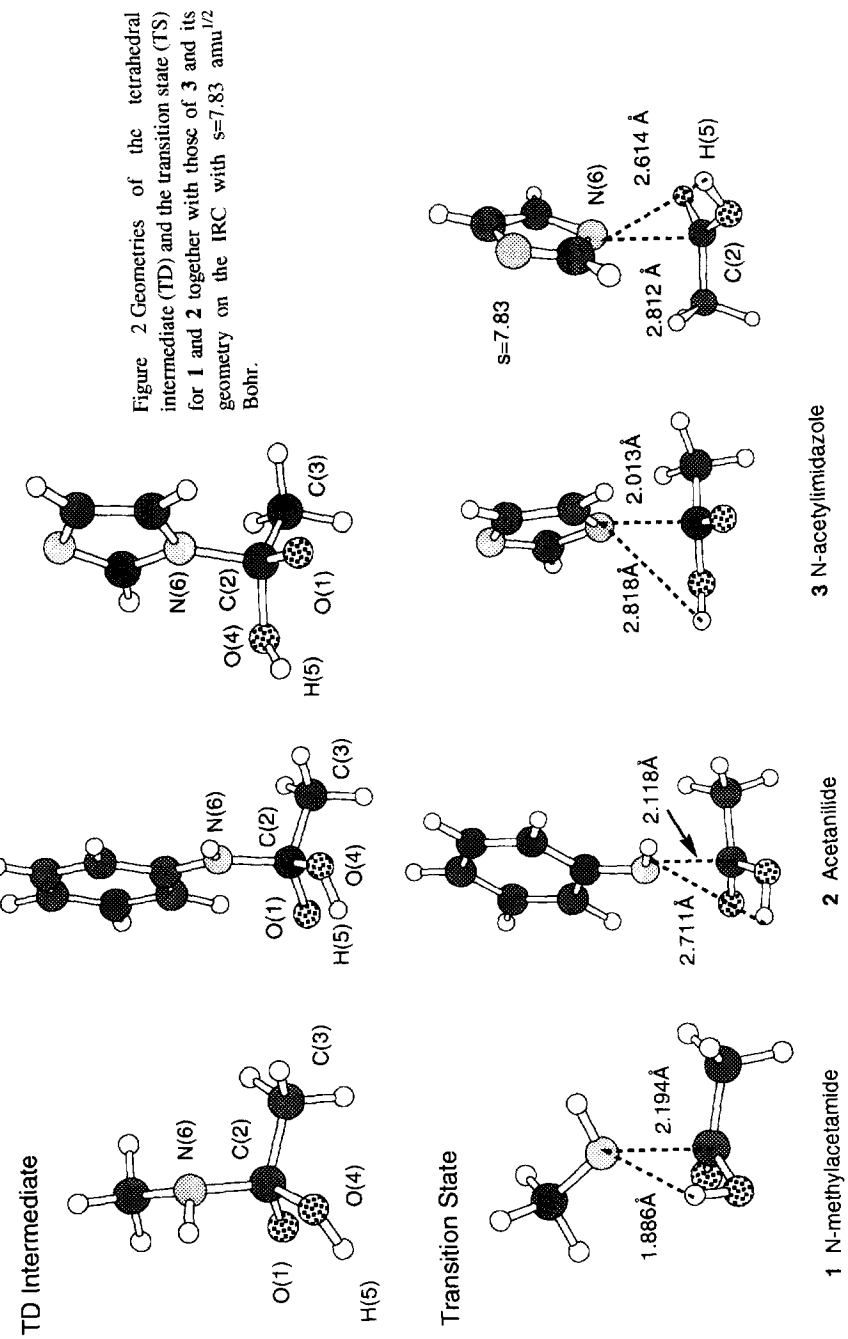

Figure 2 Geometries of the tetrahedral intermediate (TD) and the transition state (TS) for **1** and **2** together with those of **3** and its geometry on the IRC with s=7.83 amu$^{1/2}$ Bohr.

underestimated by 9.3 kcal mol^{-1} in comparison with the MP2/6-31+G*//RHF/6-31+G level which calculated the energy to be 21.4 kcal mol^{-1}. The corresponding energies for ester hydrolysis were calculated to be 25-45 kcal mol^{-1}.[1,2,3] The products of Path 1, CH_3COOH and CH_3NH^-, are unstable by ΔE_2= 47.2 (50.1) kcal mol^{-1} vis-à-vis the TD intermediate. This energy, which is much larger by ca. 20 kcal mol^{-1} than the corresponding values for esters, is considered to be the activation energy of Path 1 in the gas phase. It is, therefore, more difficult to form the Y^- anion from amide than from esters in the gas phase.

The calculation shows that the activation energy for Path 2 is ΔE_3(TS)= 21.4 (22.3) kcal mol^{-1}, which is less than half of ΔE_2. With the energy difference of 25.8 (27.8) kcal mol^{-1} between ΔE_2 and ΔE_3(TS), Path 2 for **1** is preferred to Path 1 in the gas phase. The TD intermediate decomposes into CH_3COO^- and CH_3NH_2, releasing stabilization energy that amounts to 16.1 (18.0) kcal mol^{-1}.

The calculation of the ΔE_1 for **2** turned out the value of 33.5 (24.7) kcal mol^{-1}. The MP2/6-31+G//RHF/6-31G calculations again underestimated this energy by 8.8 kcal mol^{-1} in comparison with that of MP2/6-31+G*//RHF/6-31+G calculation. The products of Path 2, CH_3COO^- and $C_6H_5NH_2$, are more stable by 7.9 (10.2) kcal mol^{-1} than the TD intermediate. ΔE_3(TS) was by estimation 8.8 (12.8) kcal mol^{-1}, which roughly half of ΔE_2 since the value for **2** was estimated to be ca. 18[20] (22.3) kcal mol^{-1}. Therefore, it is again gathered that, in the gas phase, there is a preference for Path 2 over Path 1 in the alkaline hydrolysis of acetanilide.

3 has completely different energy correlation form those for the former two amides. ΔE_1= 54.5 (45.5) kcal mol^{-1} is larger by ca. 30 kcal mol^{-1} and ΔE_2= 7.5 (13.1) kcal mol^{-1} smaller by ca. 40 kcal mol^{-1} than those of **1**. The ΔE_4 was calculated to be 4.1 (3.0) kcal mol^{-1}, i.e., the product, CH_3COO^- + imidazole, is more unstable than the TD intermediate although they are still more stable by 3.4 (10.1) kcal mol^{-1} than the other products, CH_3COOH + imidazolyl anion.

Energy Relation Including Solvent Effect

The energy relation in aqueous solution was estimated for molecules in Paths 1 and 2 by using the IPCM calculations. The ΔE_4(SCRF) for **1**, **2** and **3** are larger by -7.8, -13.4 and -17.7 kcal mol^{-1} than the corresponding values in the gas phase. The stability of the products of Path 2, CH_3COO^- + RNH_2 increases in a solution of water. As discussed above, the TD intermediates in the gas phase are more stable than the reactants for all the amide calculated here. This is not true in aqueous solution. The ΔE_1(SCRF) of **1** is -3.7 kcal mol^{-1} which is smaller by 25.1 kcal mol^{-1} than the gas phase value, i.e., the TD intermediate is less stable than reactants, **1** + OH^-. This is completely different relation from that in the gas phase as expected. It is necessary to remove solvents around the OH^- anion in aqueous solution to form the TD intermediate. It follows that the O-C bond formation and the solvation for the TD intermediate cannot fully compensate the destabilization due to desolvation of the OH^- ion. On the other hand, the TD intermediates for **2** and **3** are still more stable by 5.9 and 24.2 kcal mol^{-1} than the reactants in aqueous solution, respectively, although these values were reduced by 27.6 and 30.3 kcal mol^{-1} from the gas phase ones.

The activation barriers ΔE_3(TS,SCRF) were estimated to be 26.1, 13.2 and 4.2 kcal mol^{-1} for **1**, **2** and **3**, respectively. As these values are larger than those in the gas phase, the differences are not large (less than 5 kcal mol^{-1}) so that the aqueous environment changes the barrier height a little. It is important to point out that the relation between ΔE_2(SCRF) and ΔE_3(TS,SCRF) is dependent on a leaving group. As the ΔE_2(SCRF) of **1** was calculated to be 33.4 kcal mol^{-1}, the products of Path 1, CH_3COOH + CH_3NH^-, locate at the higher position by 7.3 kcal mol^{-1} than the TS of Path 2 even in the aqueous phase. The CH_3NH^- anion is a bad leaving

group even in a solution of water. On the other hand, the products of Path 1 of **3**, imidazolyl ion and CH_3COOH, are more stable than the TD intermediate since its ΔE_2(SCRF) is negative (-2.4 kcal mol^{-1}). This value is smaller by 6.6 kcal mol^{-1} than the ΔE_3(TS,SCRF). It is gathered that the breakdown of the TD intermediate may produce not imidazole but imidazolyl ion.

Geometry Transformation along the IRC

Next, calculations were made on the IRC's for **1**, **2** and **3** to see whether the TS geometries obtained connect the reactants and the products. Figure 3 displays the geometrical transformations for **1** along the IRC. The structure gets the closest to that of the TD intermediate at s=-5.79 $amu^{1/2}$ Bohr.[21] In the early stages of the reaction down to the TS, the breaking of the C-N bond occurs. At the TS, the H(5) atom of the OH fragment is ready to move toward the N(6) atom of the amine fragment. When the transformation reaches as far as s=2.49 $amu^{1/2}$ Bohr, the H(5) atom makes a weak bridge between the N(6) and the O(4) atom. At s=2.98, the stage where the amine fragment has completed the extraction of the light atom from the acid fragment, N-methyl amine forms. Krug et al. also obtained a similar geometry transformation along the IRC for the alkaline hydrolysis of formamide.[22] They obtained the activation barrier to be 19 kcal mol^{-1} at the MP2/6-31G*//4-31G level of theory.

It is possible to consider a hydrogen-bonded (HB) structure as one of the intermediates on a reaction coordinate. This intermediate is more stable by 28.0 kcal mol^{-1} than the TD intermediate (MP2/6-31+G//RHF/6-31G level). In the gas phase reaction, the HB intermediate, however, may not form because its geometry is dissimilar to that at s=5.98, but decompose directly into the final products, $CH_3COO^- + CH_3NH_2$.

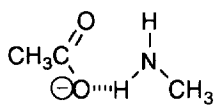

With **2**, a similar geometrical change in Figure 3 was obtained except for that the H(5) atom begins to move at the different position around 7.0 $amu^{1/2}$ Bohr on the IRC in the 6-31G level of theory as discussed below. The geometry transformation of **3** at the 6-31+G level of theory was very similar to that from the previous 6-31G calculations.[14] It is worth noting that the geometry at s=7.83 $amu^{1/2}$ Bohr in Figure 2 (the RHF/6-31+G calculation) shows the H(5)-N(6) length to be 2.614 Å although the C(2)-N(6) length is as long as 2.812 Å. It means that the TD intermediate decomposes to acetic acid and imidazolyl anion so that the TS obtained for **3** should be that for Path 1.

Potential Energy Profiles along the IRC

It is interesting to see the potential energy profile along the IRC since this factor is extremely dependent on the nature of leaving groups in parent amides. The basis set dependence of the potential energy profile were analyzed[23] since we calculated the IRC for **2** using the 6-31G basis set for the simplicity of calculations. Figure 4a shows the potential energy profiles of hydrolysis for the three amides along the IRC, where s=0.0 $amu^{1/2}$ Bohr stands for the TS. The solid and broken lines are the potential curves calculated at the RHF/6-31G and RHF/6-31+G level of theory, respectively. The shapes of the two curves for **1** and **3** are very similar although their heights are different a little. The changes of the O-H distances along the IRC also have similar trend as shown in Figure 4b. Therefore, the 6-31G calculations is qualitatively as reliable as the 6-31+G

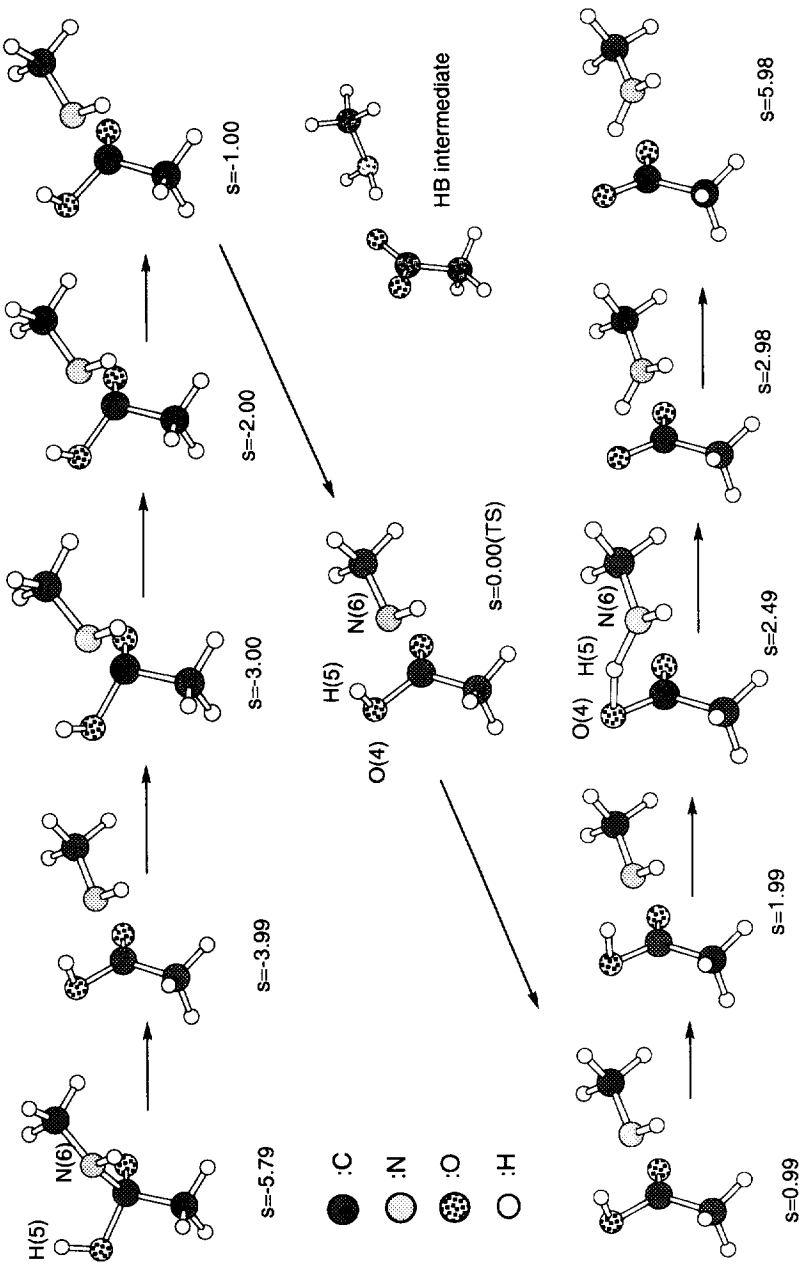

Figure 3 Geometry transforamtion along the IRC for Path 2 of **1** in the RHF/6-31+G level of theory. Values under each geometries indicate the lengths from the TS in amu$^{1/2}$ Bohr unit.

calculations. Therefore, we will discuss the results of the smaller basis sets in this section.

Each curve in Figure 4a has its own feature: the curve of **1** shoots straight up till it reaches the TS, after which it plunges; with **2** unlike **1**, the curvature draws a blunt acclivity till the TS, and thereafter it follows a gentle downward plateau where the energy is slowly reduced to s=8.0, and then it suddenly drops as seen with **1** after the TS. No such dramatic change takes place with **3**, the curve simply comprising mild dents and bumps before and after the TS. It follows, therefore, that the amides calculated differ from each other in the potential energy profiles very much.

There are other features worthy of mention in the potential curves shown in Figure 4a. Around s=-4.0 amu$^{1/2}$ Bohr, the potential curve for **3** is flat with the value of ca. 0.0 kcal mol^{-1}, suggesting that the geometry of this point is almost the same as that of the TD intermediate. The potential value of **2** at the similar point is ca. 3 kcal mol^{-1} and the extrapolation of the curve expects the value to be 0.0 kcal mol^{-1} around -5.0 amu$^{1/2}$ Bohr. The potential curve for **1** is located at ca. 8 kcal mol^{-1} in the vicinity of s= -4.0 amu$^{1/2}$ Bohr and is 0 kcal mol^{-1} close to or beyond s= -6 amu$^{1/2}$ Bohr. The calculations show that the activation energies for **3**, **2** and **1** are 5.6 (2.8), 12.8 (8.8) and 22.3 (21.4) kcal mol^{-1} at the MP2/6-31+G//RHF/6-31G (MP2//6-31+G*//RHF/6-31+G) level of theory, respectively. The horizontal axis of Figure 4 indicates distances of certain kind from the TS,[18,21] whereby the more distant the reactant is, the larger activation energy the TS has. This is consistent with the Hammond postulate.[24]

Figure 4b shows the change in the O-H distances along the IRC. As regards the change in the O-H distances, **2** resembles **1**, only differing in the positions where the distance gets to be protracted, the positions immediately after the TS with **1** and at s=7.0 amu$^{1/2}$ Bohr with **2**. In Figure 3b this remarkable change in the geometry accords with the structures at s=1.99, 2.49 and 2.98 amu$^{1/2}$ Bohr. From these geometries, we can see how the amine fragment extracts the H atom from the OH fragment. It is worth noting that the breaking of the OH bond and in turn the forming of the N-H bond accompanies the sudden decrease of the potential energies for both **1** and **2** seen in Figure 4. With **3**, within the IRC region in the figure there is no such rapid decrease in potential energy. We can thus conclude that the formation of a new N-H bond is closely related to the nature of the leaving groups.

What makes the potential energy of **2** and **3** flat after the TS? What kind of effect locates their TS position earlier than that of **1**? It is considered that the origin of the phenomena is the magnitude of the resonance

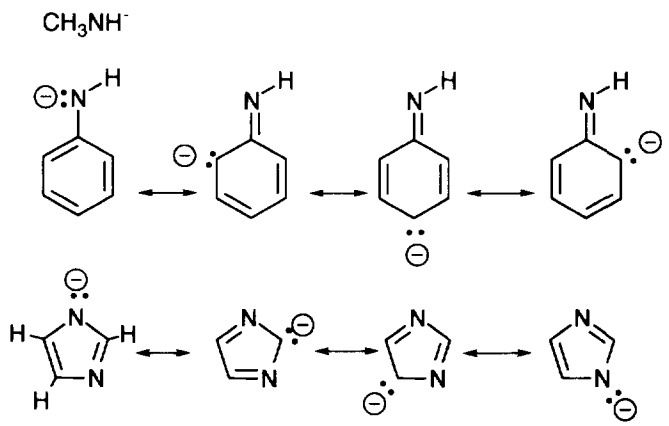

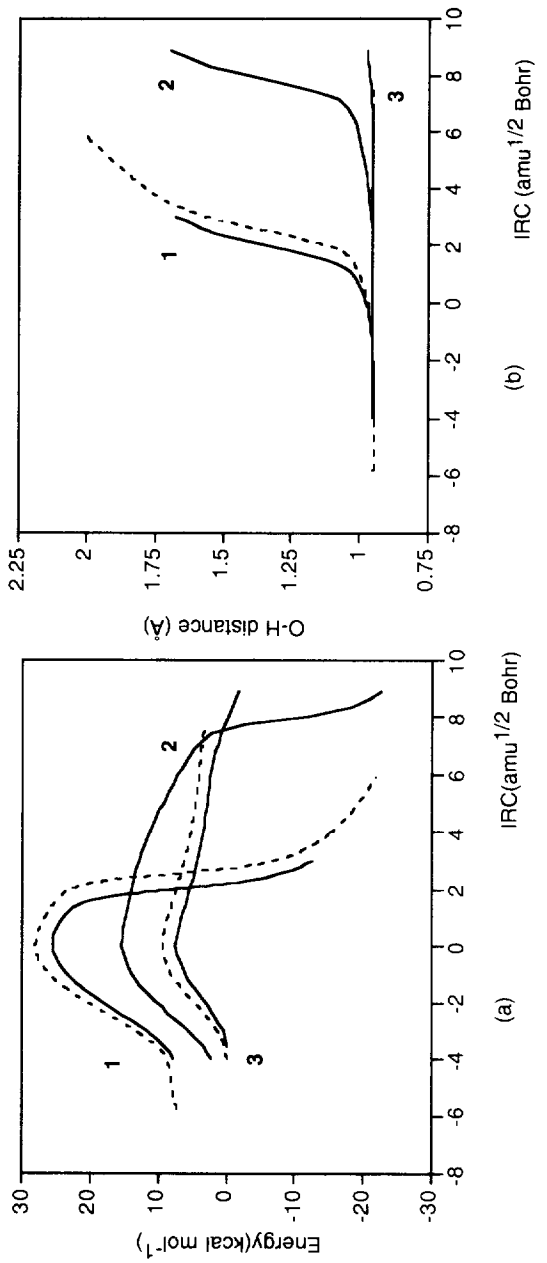

Figure 4 Potential energy profile (a) and the change of the O-H distances (b) along the IRC for the breakdown of the TD intermediates of **1**, **2**, and **3**. The solid and broken lines show the results from the IRC calculations using the 6-31G and 6-31+G basis sets, respectively.

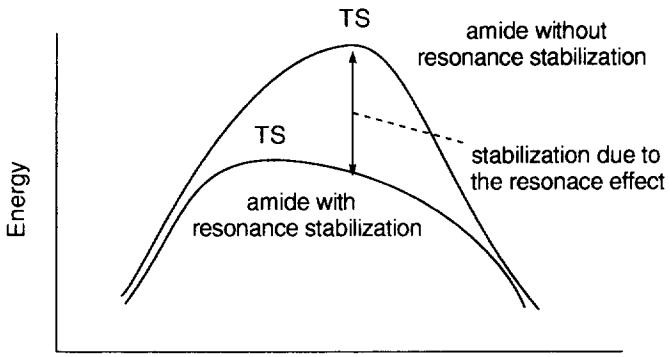

Figure 5 Schematic representation of the change in the potential energy profile caused by the resonance effect.

effect in the leaving anions. Imidazolyl and $C_6H_5NH^-$ anions are considered to have several resonance structures, and the CH_3NH^- anion has no such structures. The magnitude of ΔE_5 (Table 2), the energy difference between Y^- and YH in the gas phase, is an indicator of the resonance effect. The calculated values are 411.8, 376.2 and 353.8 kcal mol^{-1} in the MP2/6-31+G//RHF/6-31G level of theory, respectively, in accord with the anticipated resonance stabilization of the anions.

The leaving group CH_3NH^- in **1** contains no resonance stabilization, and the destabilization of the system occurs during the breaking of the C-N bond. It is by the transfer of the H atom from the OH to the amine fragment, i.e., the formation of the new N-H bond, that the system is stabilized. It has to remind that the light atom is ready to leave for the amine fragment at the TS of **1** shown in Figure 3, while, on the other hand, in the cases of **2** and **3** the resonance effect compensates the destabilization caused by the breaking of the C-N bond shown in Figure 5. This effect puts the TS position in an earlier stage of the reaction and lowers the activation energy. However, the resonance effect is not enough to form $C_6H_5NH^-$ as one of the products for the hydrolysis for **2**. The imidazolyl anion, because it has large resonance effect, is not so much destabilized as the rest. This fact means that imidazolyl anion has the weak Lewis basicity, hence it cannot extract the H atom from the OH fragment.

Concluding Remarks

The mechanisms of alkaline hydrolysis for the three amides were investigated by using *ab initio* MO calculations. It is ascertained that, in the gas phase, Path 2 vis-à-vis Path 1 is a better route to decompose the TD intermediate for **1** and **2**. The SCRF calculations indicated that Path 2 for **1** is also a better route than Path 1 even in aqueous solution. In the present study, we did not estimate how a solvent water as a reactant assists to reduce the activation energy of Path 1. As far as these amides are concerned, the resonance effect is not enough to stabilize the anions, CH_3NH^- and $C_6H_5NH^-$, and therefore, CH_3COO^- and YH directly form as the products. On the other hand, the resonance effect stabilizes the imidazolyl anion enough to make the alkaline hydrolysis of N-acetylimidazole to release an acetic acid and imidazolyl anion, which are more stable than the TD intermediate in aqueous solution. Therefore, the ability as the leaving group determines which mechanism

is favorable for the alkaline hydrolysis. It is a common knowledge that the alkaline hydrolysis of *p*-substituted acetanilide depends on the electron-withdrawing ability attributed to the substituents,[6,7,8] i.e., the magnitude of the resonance effect discussed above.

Acknowledgment

The authors owe thanks to the Computer Center, Institute for Molecular Science at the Okazaki National Research Institutes for the use of the NEC HSP computers and the Library Program GAUSSIAN92. This work is supported by the Grant-in-Aid for Scientific Research from the Ministry of Education of Japan.

References and Notes

1. Madura, J. D.; Jorgensen, W. L. *J. Am. Chem. Soc.*, **1986**, 108, 2517

2. Hori, K. *J. Chem. Soc. Perkin Trans. 2.* **1992**, 1629.

3. Ewig, C. S.; Van Wazer, J. R. *J. Am. Chem. Soc.*, **1986**, 108, 4774

4. (a) Takashima,K.; Jose,S. M.; do Amaral, A. T; Riveros, J. M. *J. Chem. Soc. Chem. Commun.*, **1983**, 1255 (b) Faigle, J. F. G.; Isolani, P. C.; Riveros, J. M. *J. Am. Chem. Soc.*, 1976, **98**, 2049 (c) Takashima, K.; Riveros, *J. Am. Chem. Soc.*, J. M., 1978, **100**, 6128

5. For Example, J. March, "Advanced Organic Chemistry", John Wiley & Sons, 1992, pp338-341

6. (a) Biechler, S. S.; Taft, Jr., R. W. *J. Am. Chem. Soc.*, **1957**, 79, 4927 (b)Bender, M. L.; Thomas, R. J. *J. Am. Chem. Soc.*, **1961**, 83, 4183 (c) Pollack, R. M.; Bender, M. L. *J. Am. Chem. Soc.*, **1970**, 92, 7190 (d) Gani, V.; Viout, P. *Tetrahedron*, **1976**, 32, 1669

7. (a) Mader, P. M.; *J. Am. Chem. Soc.*, **1965**, 87, 3191 (b) Schowen, R. L.; Jayaraman, H.; Kershner, L. *J. Am. Chem. Soc.*, **1966**, 88, 3373 (c) Schowen, R. L.; Jayaraman, H.; Kershner, L.; Zuorick, G. W. *J. Am. Chem. Soc.*, **1966**, 88, 4008 (d) Eriksson, S. O. *Acta Chem Scand.*, **1968**, 22, 892 (e) Kershner, L. D.; Schowen, R. L. *J. Am. Chem. Soc.*, **1971**, 93, 2014

8. (a) Bender, M. L. *J. Am. Chem. Soc.*, **1951**, 73, 1626 (b) Bender, M. L.; Ginger, R. D.; Kemp, K. C. *J. Am. Chem. Soc.*, **1954**, 76, 3350 (c) Bunton, C. A.; Nayak, B.; O'Connor, C. J. *J. Org. Chem.*, **1968**, 33, 572

9. Slebocka-Tilk, H.; Brown, R. S. *J. Org. Chem.*, **1988**, 53, 1153

10. (a) DeRoo, M.; Bruylants, A. *Bull. Soc. Chim. Belg.*, **1954**, 63, 140 (b) Calvet, E. *J. Chim. Phys.*, **1933**, 30, 140

11. (a) Slebocka-Tilk, H.; Bennet, A. J.; Keillor, J. W.; Brown, R. S.; Guthrie, J. P.; Jodhan, A. *J. Am. Chem. Soc.*, **1990**, 112, 8507 (b) Slebocka-Tilk, H.; J. Bennet, A.; Hogg, H. J.; Brown, R. S. *J. Am. Chem. Soc.*, **1991**, 113, 1288 (c) Brown, R. S.;Bennet, A. J. ; Slebocka-Tilk, H. *Acc. Chem. Res.*, **1992**, 25, 481 (d) Brown, R. S.; Bennet, A. J.; Slebocka-Tilk, H.; Jodhan, A. *J. Am. Chem. Soc.*, **1992**, 114, 3092

12. (a) Alagona, G.; Scrocco, E.; Tomasi, J. *J. Am. Chem. Soc.*, **1975**, 97, 6976 (b) Oie, T.; Loew, G. H.; Burt, S. K.; Binkley, J. S.; MacElroy, R. D. *J. Am. Chem. Soc.*, **1982**, 104, 6169 (c) Jensen, J. H.;

Baldridg, K.K; Gordon, M. S. *J. Phys. Chem.*, **1992**, 96, 8340 (d) Antonczak, S.; Ruiz-López, M. F.; Rivail, J. L. *J. Am. Chem. Soc.*, **1994**, 116, 3912

13. Foresman, J. B.; Frish, Æ. "*Exploring Chemistry with Electronic Structure Methods: A Guide to Using Gaussian*" Gaussian, Inc., 1996, Chapter 10

14. Hori, K.; Kamimura, A.; Kimoto, J.; Gotoh, S.; Ihara, Y. *J. Chem. Soc. Perkin Trans. 2*, **1994**, 2053

15. (a) MOPAC Ver.6., Stewart, J. J. P. QCPE Bull., **1989**, 9, 10. (b) We performed semi-empirical PM3 calculations, and then, the obtained PM3 geometries were used as the initial geometries of the *ab initio* calculations. Although the PM3 geometries were not far from the 6-31+G geometries, the semi-empirical calculation did not represent well the energy relation among reactants, intermediates, products and TS.

16. Gaussian 94, Revision C.2, Frisch, M. J.; Trucks, Schlegel, H. B.;G. W.; Gill, Johnson, B. G.; Robb, M. A.; Cheeseman, J. R.; Keith, T.; Petersson, G. A.; Montgomery,J. A.; Raghavachari,K.; Al-Laham, M. A.; Zakrzewski,V. G.; Ortiz,J. V.; Foresman,J. B.; Cioslowski, J.; Stefanov, B. B.; Nanayakkara, A.; Challacombe, M.; Peng, C. Y.; Ayala, W.; Chen, P. Y.; Wong,M. W.; Andres, J. L.; Replogle, E. S.; Gomperts, R.; Martin, R. L.; Fox, D. J.; Binkley, J. S.; Defrees, D. J.; Baker, J.; Stewart, J. J. P.; Head-Gordon, M.; Gonzalez, C.; Pople, J. A. Gaussian, Inc., Pittsburgh PA, 1995.

17. Hehre, W. J.; Ditchfield, R.; Pople, J. A. *J. Chem. Phys.*, **1972**, 56, 2257.

18 (a) Fukui, K. *Acc. Chem. Res.*, **1981**, 14, 363 (b). Head-Gordon, M; Pople, J. A. *J. Chem. Phys.*, **1988**, 89, 5777

19 Values are the geometrical parameters or energies from the 6-31+G (6-31G) level calculations.

20. We could not obtained the optimized geometry of $C_6H_5NH^-$ with the RHF/6-31+G level of theory because of the SCF convergence failure. Table 2 shows the MP2/6-31+G//RHF/6-31G calculations overestimated ΔE_2 for **1** and **3** by 3-5 kcal mol^{-1} in comparison with those at the MP2/6-31+G*//RHF/6-31+G level of theory. As the smaller basis set calculation gave ΔE_2 for **2** to be 22.3 kcal mol^{-1}, we can roughly estimate that value to be ca. 18 kcal mol^{-1}.

21. "s" in amu$^{1/2}$ Bohr unit is a kind of the distance from the TS, showing how a geometry on the IRC is different from the TS geometry. The potential energy profile from the IRC calculation is completely different from that of the minimum energy path, which is obtained by a series of geometry optimization with a fixed parameters such as the C-N length. No geometrical parameters have constant increment or decrement of their values along the IRC.

22. Krug,J. P.; Popelier, P. L. A.; Bader, R. F. W. *J. Phys. Chem.*, **1992**, 96, 7604

23. We also have done the calculations including the correlation effect for optimization TD, TS geometries for **1** at the MP2/6-31+G level of theory. The IRC calculation showed that the TS geometry also similarly connected the TD intermediate with the products, CH_3COO^- and CH_3NH_2. The MP2/6-31+G energies are -322.95703 and -322.92960 Hartree for the TD and TS, respectively. The activation energy is estimated to be 17.2 kcal mol^{-1}, which is smaller a little than that at the MP2/6-31+G*//RHF/6-31+G level of the theory.

24. Hammond, G. S. *J. Am. Chem. Soc.*, **1955**, 77, 334

(*Received in Japan* 22 *November* 1996; *accepted* 10 *February* 1997)